Science in China Series B: Chemistry

www.scichina.com
chem.scichina.com
www.springerlink.com

Hydrogen bonding of single acetic acid with water molecules in dilute aqueous solutions

PU Liang[1, 2], SUN YueMing[1†] & ZHANG ZhiBing[2†]

[1] School of Chemistry and Chemical Engineering, Southeast University, Nanjing 211189, China;
[2] Separation Engineering Research Center of Nanjing University, Key Laboratory in Meso- & Microscopic Chemistry of Ministry of Education of China, School of Chemistry and Chemical Engineering, Nanjing University, Nanjing 210093, China

In separation processes, hydrogen bonding has a very significant effect on the efficiency of isolation of acetic acid (HOAc) from HOAc/H_2O mixtures. This intermolecular interaction on aggregates composed of a single HOAc molecule and varying numbers of H_2O molecules has been examined by using *ab initio* molecular dynamics simulations (AIMD) and quantum chemical calculations (QCC). Thermodynamic data in aqueous solution were obtained through the self-consistent reaction field calculations and the polarizable continuum model. The aggregation free energy of the aggregates in gas phase as well as in aqueous system shows that the 6-membered ring is the most favorable structure in both states. The relative stability of the ring structures inferred from the thermodynamic properties of the QCC is consistent with the ring distributions of the AIMD simulation. The study shows that in dilute aqueous solution of HOAc the more favorable molecular interaction is the hydrogen bonding between HOAc and H_2O molecules, resulting in the separation of acetic acid from the HOAc/H_2O mixtures with more difficulty than usual.

acetic acid, hydrogen bond, *ab initio*, molecular dynamics, free energy

1 Introduction

In modern chemical processing, distillation is widely used in the separation of acetic acid (HOAc) from HOAc/H_2O mixtures to obtain acetic acid (HOAc) of various purities. However, in practical processing, there is always the problem of low distillation efficiency, especially for very dilute solutions. This problem causes frustrations and failures in industrial distillation tower design and requires revamping the separation system. One of the crucial reasons is the hydrogen bonding (H-bonding), which acts as the strongest force governing the physical and chemical properties of the mixtures, including the vapor-liquid equilibrium of the HOAc/H_2O system.

The HOAc molecule has hydrophobic (methyl) and hydrophilic (carboxyl) sites. Except under extremely high pressure, interactions involving the methyl groups are rather weak under most conditions[1], while the carbonyl and hydroxyl are both active and form hydrogen bonds (H-bond) with each other. This feature leads the HOAc to form a cyclic dimer in most phases, such as gas[2,3], some nonpolar solvents[4−6], and pure liquid[7]. As in aqueous solutions, an equilibrium between monomeric HOAc and its cyclic dimer was found and characterized by a dimerization constant K_D[8−12]. Recently, Johnson et al.[13,14] attributed the observed vibrational sum frequency spectra (especially of HOAc/H_2O solutions with high acid concentrations) to several species including the HOAc cyclic dimer. Moreover, Nishi et al.[15] suggested the dominant species are large aggregates of HOAc molecules, which produce microphases.

Received July 16, 2009; accepted September 8, 2009
doi: 10.1007/s11426-009-0288-4
†Corresponding author (email: sun@seu.edu.cn, segz@nju.edu.cn)
Supported by the Jiangsu Planned Projects for Postdoctoral Research Funds (No. 0901001C), the National Natural Science Foundation of China (Grant No. 20876072) and the Natural Science Foundation of Jiangsu Province (No. KB2008023)

By contrast, some other studies have suggested that the favorable structures are aggregates of HOAc and water molecules rather than the HOAc cyclic dimer[16−18], and especially in dilute solutions the interactions between the HOAc and water molecules become more competitive[10,11]. The attenuated total reflection-infrared (ATR–IR) and Raman spectra of CH_3COOD and CD_3COOD in D_2O solution measured by Génin et al.[19] indicate that aggregates of a single HOAc and varying water molecules are the only species present in 0.1−1 mol·L^{-1} solutions. Using large-angle X-ray scattering and NMR techniques, Takamuku et al.[20] suggested that when HOAc mole fraction x_A decreases, H-bonds between HOAc and water will gradually increase, and when $x_A \leqslant$ ~0.18, water clusters will predominate in the HOAc/H_2O mixtures. Recently, by using the high-resolution microwave spectroscopic method, Ouyang et al.[21] confirmed the presence of the monohydrate and dihydrate of acetic acid.

In our previous work[22,23], the dominant molecular aggregates in dilute aqueous solution of HOAc tended to be those composed of both the HOAc and water molecules rather than the acetic acid clusters. The geometries and energies derived by quantum chemical calculations (QCC) in that work were in gas phase. In the present work, our study has taken the solvent effects into consideration and extended the calculations to aqueous solutions. The derived geometries, energies and thermodynamic properties in the aqueous system will be compared to the results of QCC in gas phase and the *ab initio* molecular dynamics simulations (AIMD)[24].

2 Computational methods

2.1 AIMD

By using the CPMD package[25], the AIMD simulations were carried out on two systems composed of 1 or 2 HOAc molecules and 20 water molecules in the NPT ensemble (with a constant pressure of 1 bar, a constant temperature of 300 K, and an average density of 1.0 g·cm^{-3}). The structure with the single HOAc molecule was labeled as 1A20W, and the one with double HOAc molecules was named as 2A20W. The gradient-corrected Becke, Lee, Yang, and Parr (BLYP)[26,27] exchange correlation functional was employed. The Kohn–Sham orbitals were expanded in a plane wave basis set with a cutoff of 70 Ry. The fictitious electron mass was 1100 a.u. The time step was set at 7 a.u. (0.169 fs), and the trajectory data were collected every 10 steps. When the system has equilibrated for 1.69 ps, the simulation was run for approximately 16.9 ps.

2.2 QCC

Following previous approaches[28,29], we can estimate the aggregation Gibbs free energy of each aggregate in aqueous solution. The aggregation of a single HOAc molecule and varying water molecules can be illustrated by:

$$\mathrm{HOAc(gas)} + \mathrm{(H_2O)}_n\mathrm{(aq)} \rightarrow \mathrm{HOAc\cdot(H_2O)}_n\mathrm{(aq)} \quad (1)$$

The aggregation free energy, $\Delta G_{agg}[\mathrm{HOAc\cdot(H_2O)}_n]$, is then derived by:

$$\begin{aligned}&\Delta G_{agg}\left[\mathrm{HOAc\cdot(H_2O)}_n\mathrm{(aq)}\right]\\ &= G\left[\mathrm{HOAc\cdot(H_2O)}_n\mathrm{(aq)}\right] - G\left[\mathrm{HOAc(gas)}\right]\\ &\quad - G\left[\mathrm{(H_2O)}_n\mathrm{(aq)}\right]\end{aligned} \quad (2)$$

Obviously, the Gibbs free energies of HOAc (gas), $(H_2O)_n$(aq) and HOAc·$(H_2O)_n$(aq) are needed. The free energy in gas phase can be obtained by frequency calculations and that in aqueous solution can be calculated by summing up the free energy of the corresponding aggregate in gas phase and that of the bulk solvent shift:

$$G\left[\mathrm{(H_2O)}_n\mathrm{(aq)}\right] = G\left[\mathrm{(H_2O)}_n\mathrm{(gas)}\right] + \Delta G_{sol}\left[\mathrm{(H_2O)}_n\right] \quad (3)$$

$$\begin{aligned}&G\left[\mathrm{HOAc\cdot(H_2O)}_n\mathrm{(aq)}\right]\\ &= G\left[\mathrm{HOAc\cdot(H_2O)}_n\mathrm{(gas)}\right] + \Delta G_{sol}\left[\mathrm{HOAc\cdot(H_2O)}_n\right]\end{aligned} \quad (4)$$

Then, the aggregation free energy, $\Delta G_{agg}[\mathrm{HOAc\cdot(H_2O)}_n\mathrm{(aq)}]$, can be estimated via

$$\begin{aligned}&\Delta G_{agg}\left[\mathrm{HOAc\cdot(H_2O)}_n\mathrm{(aq)}\right]\\ &= \Delta G_{gas}\left[\mathrm{HOAc\cdot(H_2O)}_n\right] + \Delta\Delta G_{sol}\left[\mathrm{HOAc\cdot(H_2O)}_n\right]\end{aligned} \quad (5)$$

Therein, $\Delta G_{gas}[\mathrm{HOAc\cdot(H_2O)}_n] = G[\mathrm{HOAc\cdot(H_2O)}_n\mathrm{(gas)}] - G[\mathrm{(H_2O)}_n\mathrm{(gas)}] - G[\mathrm{HOAc(gas)}]$, which is the aggregation free energy in gas phase, and $\Delta\Delta G_{sol}[\mathrm{HOAc\cdot(H_2O)}_n] = \Delta G_{sol}[\mathrm{HOAc\cdot(H_2O)}_n] - \Delta G_{sol}[\mathrm{(H_2O)}_n]$, which is the bulk solvent shift from the gas phase to the aqueous solution.

To calculate the free energies in gas phase (ΔG_{gas}), the structures of various aggregates with a single HOAc molecule and varying H_2O molecules (from 1 to 4) were first optimized in gas phase and then the frequency cal-

culations were carried out to obtain the thermodynamic properties in gas phase. To obtain the free energies of solvation (ΔG_{sol}), self-consistent reaction field (SCRF) calculations were performed in aqueous solution, employing the polarizable continuum model (PCM) which used the integral equation formalism variant (IEFPCM)[30−32]. Zhan et al.[28] suggested that the effect of bulk solvent using geometries optimized in different environment was negligible. To confirm this, we performed two calculations using the geometries of the gas phase and those re-optimized geometries in aqueous environment. Both results will be presented.

All the calculations were performed at the MP2/6-31+G(d,p) level by using Gaussian 98 or 03 programs[33,34]. Calculation of the binding energies (ΔE) included counterpoise correction of the basis set superposition error (BSSE)[35]. The ring size was derived by counting the number of heavy atoms. The ring on the carboxylic acid side is called the head-on ring and that on the methylcarbonyl side or the methyl–hydroxyl side is called the side-on ring.

3 Results and discussion

3.1 AIMD

Gao et al.[36] and Pu et al.[22] recently reported H-bonding involving a single HOAc and several water molecules, in which the dominant structures were found to be the aggregates with head-on rings. By the same method[37], we obtained from the AIMD simulations the size distributions of the head-on rings which involve the single HOAc molecule (shown in Figure 1). There are three distributions: one involves a single HOAc molecule of 1A20W and the other two involve that of 2A20W. The two HOAc molecules of 2A20W were labeled as HOAc α and HOAc β, respectively, just to distinguish them, without any practical meaning. Note that the ring distributions relate to all the configurations of the 16.9 ps production. The statistics show that for 1A20W at least 22.0% of the configurations contain head-on rings, while for 2A20W, up to 12.3% of the configurations involving HOAc α and 30.6% of that involving HOAc β contain the head-on ring structures.

In Figure 1 the most evident common feature of all the three distributions is that the number of the 6-membered rings is the largest. The percentage of the 6-membered rings in the two molecules of 2A20W is larger

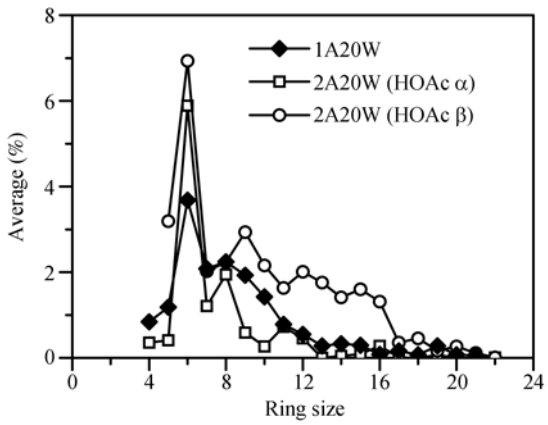

Figure 1 Distributions of the hydrogen bonded head-on rings involving a single HOAc molecule obtained from the AIMD simulations.

than that of 1A20W, and almost twice as large as that of the second most dominant ring. These results suggest that the 6-membered head-on ring with a single HOAc molecule is the dominant structure in dilute aqueous solutions of HOAc.

Recently, the planar ring structures of the HOAc monohydrate and dihydrate were confirmed by a high-resolution microwave spectroscopic method[21]. These two structures can also be found in Figure 1: the 4- and 5-membered rings. The two rings appear to be few for 1A20W (~1.0%) and HOAc α of 2A20W (~0.3%—0.4%); for HOAc β of 2A20W, there is no 4-membered ring but relatively more 5-membered rings (~3.2%). Next to the 6-membered ring, the next most dominant rings in size for 1A20W and HOAc α of 2A20W are the 7- and 8-membered rings, while the distribution of other structures above the 10-membered ring is less than 1%. For HOAc β of 2A20W, the range of the ring size is wider than that of HOAc α, with more than 1% for any structure whose ring size is less than 17, and in particular, both 5- and 9-membered rings appear to occupy about 3%.

3.2 QCC

3.2.1 Equilibrium structures. The structures of the 4-, 5-, 6- and 7-membered head-on rings in gas phase were obtained by QCC and are shown in Figure 2. According to Zhan et al.[28], the effect of bulk solvent using the geometries optimized in gas phase and aqueous environment was negligible. To confirm this, we have re-optimized the equilibrium structures of the gas phase in aqueous environment and present the corresponding results in the parentheses in Figure 2. Previ ous work has

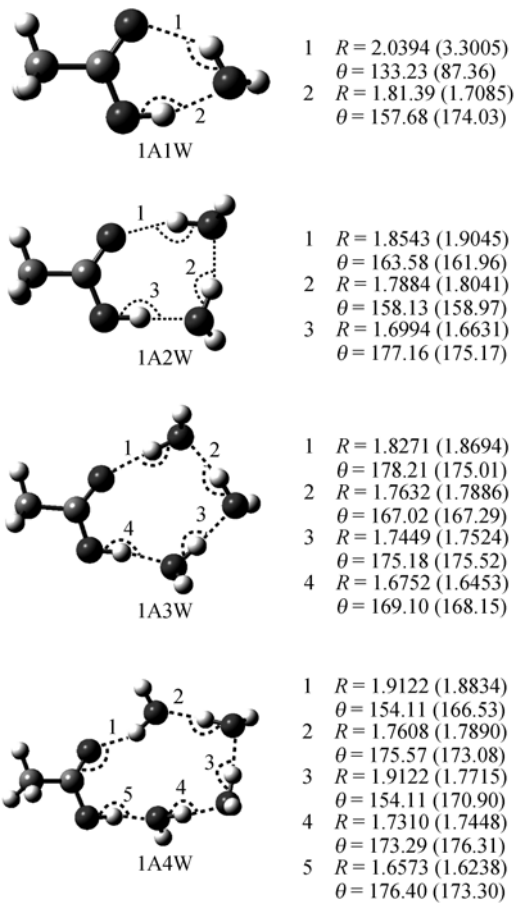

Figure 2 Equilibrium structures of the aggregates with a single HOAc and water molecules involving 4-, 5-, 6- and 7-membered head-on rings. The hydrogen bonds are marked as dashed lines, and the corresponding values, the length R in Å and the angle θ in degrees are also given. The data outside the parentheses are in gas phase, while those in the parentheses are in aqueous solutions.

pointed out that in each group with the same number of acid and water molecules, the biggest head-on ring is generally the most stable structure, with the exception of the 7-membered ring[22]. Therefore, in Figure 2, 1A1W, 1A2W and 1A3W are the dominant structures in their respective groups while 1A4W is not. The structures of the 4- and 5-membered rings are consistent with those confirmed experimentally by Ouyang et al[21].

Figure 2 shows that the H-bonds between HOAc and water molecules in the 6-membered head-on ring in 1A3W are generally shorter and more collinear than those in the 4-membered ring in 1A1W and those in the 5-membered ring in 1A2W. For the 7-membered ring in 1A4W, the H-bond between the hydroxyl and water molecules is slightly shorter and more collinear than that of the 6-membered ring in 1A3W, but the H-bond between the carbonyl and water molecules is a little longer and less collinear. Previous study has also suggested that for configurations with 4 water molecules, the 7-membered head-on ring is less stable than the 5-membered one[22]. All these facts indicate that the 6-membered head-on ring is geometrically predominant.

When the optimized geometries in the gas phase are compared with those in the aqueous system, an obvious difference in 1A1W and a slight difference in the others can be seen. For 1A1W, the H-bond between the carbonyl and water molecules in gas phase is totally broken in aqueous solution, while the H-bond between the hydroxyl and water molecules gets shorter and much more collinear. Generally, for all the aggregates except 1A4W transformed from gas phase to aqueous environment, the H-bond between hydroxyl H and water O atoms appears to be shorter in length and stronger in force, while an opposite change occurs in the H-bond between carbonyl O and water H atoms. For 1A4W, both H-bonds between HOAc and H_2O are strengthened in the process. These results indicate that the effect of the bulk solvent on the geometries cannot be completely neglected. Therefore, both geometries were used to calculate the solvation free energy (ΔG_{sol}).

The equilibrium structures of the predominant water aggregates in gas phase (those outside the parentheses) and aqueous system (those in the parentheses) are shown in Figure 3. The water dimer is linear, the trimer has a 3-membered ring, and the tetramer involves a 4-membered ring. In the aggregation process shown by equation 1, the most stable structure of the water cluster $[(H_2O)_n]$ was used. That is, in aggregation free energy calculation, the geometrical data of the water cluster are those shown in Figure 3. It can also be seen from Figure 3 that the values are very close for the geometries of the gas phase and the aqueous environment, which is consistent with Zhan's discovery[28]. However, as was mentioned above, the solvent effect on the HOAc/H_2O aggregates cannot be neglected. Therefore, both geometries were used in the solvation free energy calculations.

3.2.2 Aggregation free energies. Table 1 presents the thermodynamic results of the gas phase at 298 K and 1 atm, including the binding energies, enthalpies and free energies of the aggregates in Figure 2. It is found that the binding energy becomes more negative as the ring grows bigger because more H-bonds are formed. Aggregate 1A3W shows the lowest value for the

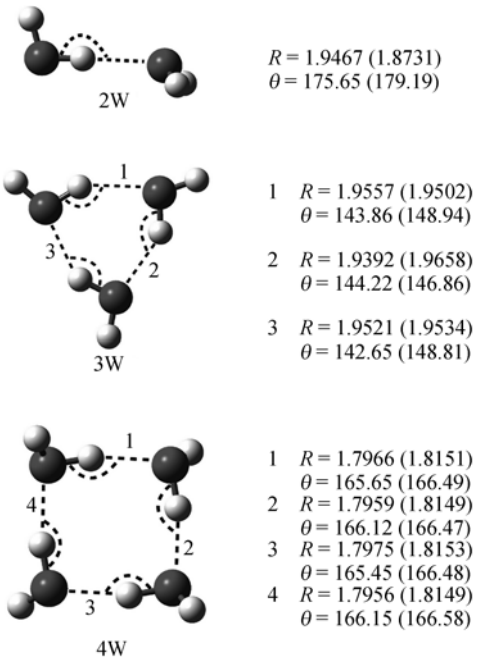

Figure 3 Equilibrium structures of the water aggregates involving 2, 3 and 4 molecules. The hydrogen bonds are marked as dashed lines, and the corresponding values, the length R in Å and angle θ in degrees, are also given. The data outside the parentheses are in gas phase while those in the parentheses are in aqueous solution.

free energies, indicating that the 6-membered ring in 1A3W is the most stable structure in gas phase. This is consistent with the distributions in the AIMD simulations, where the 6- membered ring dominates the ring. In addition, the aggregation free energy shows that in gas phase the 5-membered ring (1A2W) is quite stable while the 4-membered (1A1W) and the 7-membered rings (1A4W) seem relatively unstable.

Table 1 The binding energies, enthalpies, and free energies (T = 298 K, P = 1 atm, all in kJ·mol^{-1}) of the aggregates with one HOAc and varying water molecules in gas phase

Structure	ΔE_{gas}	ΔH_{gas}	ΔG_{gas}
1A1W	–38.702	–38.306	–0.473
1A2W	–84.548	–64.319	–14.847
1A3W	–119.228	–54.545	–20.043
1A4W	–148.419	–40.527	–6.829

Table 2 presents the solvation free energies in water and the aggregation free energies of the aggregates, using both the geometries in gas phase (the values outside the parentheses) and in aqueous environment (the values in the parentheses). No matter which geometry is used, the aggregation free energy of 1A3W (ΔG_{agg}[HOAc·$(H_2O)_3$(aq)]) is always the most negative. In gas phase,

Table 2 Estimates of the free energies of solvation in water (ΔG_{sol}) and the aggregation free energies (ΔG_{agg}) of various clusters, using the geometry in the gas phase (the values outside the parentheses) and the re-optimized one in aqueous solution (the values in the parentheses). All the energies are in kJ·mol^{-1}

Structure	ΔG_{sol}	ΔG_{agg}
A	–34.602 (–37.530)	
W	–30.711 (–31.464)	
2W	–46.568 (–48.995)	
3W	–38.744 (–40.125)	
4W	–40.920 (–43.012)	
1A1W	–25.522 (–44.643)	4.716 (–13.652)
1A2W	–29.162 (–31.798)	2.558 (2.349)
1A3W	–34.058 (–37.154)	–15.357 (–17.072)
1A4W	–38.200 (–43.639)	–4.109 (–7.457)

1A3W also has the lowest free energy (see Table 1). In the AIMD simulations, the 6-membered ring dominates the ring distributions as is shown in Figure 1. All these results suggest that in either gas phase or aqueous environment, the 6-membered ring is the most stable structure in aggregates involving one HOAc and varying water molecules.

From the ring distributions in the AIMD simulation in Figure 1, for 1A20W and HOAc α of 2A20W, the number of the rings from the 4- to 7-membered follows the trend 6 > 7 > 5 > 4. A similar trend is also found in the free energies in gas phase (ΔG_{gas}) calculated by the QCC, except that the value of the 5-membered ring in 1A2W is lower than that of the 7-membered ring in 1A4W. As to the aggregation free energies (ΔG_{agg}) in aqueous environment, the result of those using the optimized geometry of the gas phase corresponds well to that of the AIMD simulations. The similar case of ΔG_{agg} is found with those using the re-optimized geometry of the aqueous solution except that the value of the 4-membered ring is lower than that of the 7-membered ring. This is because in aqueous environment the geometry of 1A1W is no longer a 4-membered ring but a linear one, as is shown in Figure 2. It indicates that both the solvation and aggregation free energies of 1A1W using the geometry in gas phase differ significantly from those with the geometry re-optimized in aqueous solution. The value of ΔG_{agg} of the former is even positive while that of the latter is quite negative. This suggests that the 4-membered ring is unfavorable in aqueous solution and tends to be replaced by aggregates involving more water molecules. As for the 5-membered ring, though there is no significant difference between its geometries in gas

phase and in aqueous solution, the aggregation free energy indicates that it is still rather unstable in aqueous solution. The stability of the 4- and 5-membered rings is well reflected in the ring distributions of the AIMD simulation (see Figure 1). In conclusion, the changing trend of the aggregation free energy of various aggregates obtained by the QCC method is consistent with the ring distributions of the AIMD simulation.

4 Conclusions

In summary, both the dynamic and the static *ab initio* methods show that structures involving one acetic acid in aqueous solution tend to form H-bonded head-on rings. In particular, the geometries as well as the Gibbs free energies of aggregation show that the 6-membered head-on ring is the predominant aggregate, corresponding to the ring distribution of the AIMD simulations. The structures of the 4- and the 5-membered rings are consistent with those reported in the recent experimental work[21]; however, they are not very stable in aqueous solution. The dominant molecular interactions in dilute aqueous solutions of HOAc are those between HOAc and water molecules, but it is totally different from the case in more concentrated solutions, where the leading role is played by the acid aggregates[15,19,20]. Therefore, much more efforts are needed to isolate acetic acid from dilute aqueous solutions of HOAc.

We are grateful to the High Performance Computing Center of Nanjing University for awarding CPU hours to accomplish this work. We also thank Dr. Yong Zhang at University of Utah, USA, for his helpful comments and suggestions.

1 Chang H C, Jiang J C, Lin M S, Kao H E, Feng C M, Huang Y C, Lin S H. On the search for C-H-O hydrogen bonding in aqueous acetic acid: Combined high-pressure infrared spectroscopy and *ab initio* calculations study. J Chem Phys, 2002, 117: 3799－3803[DOI]
2 Karle J, Brockway L O. An electron-diffraction investigation of the monomers and dimers of formic, acetic and trifluoroacetic acids and the dimer of deuterium acetate. J Am Chem Soc, 1944, 66: 574－584[DOI]
3 Frurip D J, Curtiss L A, Blander M. Vapor phase association in acetic and trifluoroacetic acids. Thermal conductivity measurements and molecular orbital calculations. J Am Chem Soc, 1980, 102: 2610－2616[DOI]
4 Davis J C Jr, Pitzer K S. Nuclear magnetic resonance (NMR) studies of hydrogen bonding. I. Carboxylic acids. J Phys Chem, 1960, 64: 886－892[DOI]
5 Waldstein P, Blatz L A. Low-frequency Raman spectra and molecular association in liquid formic and acetic acids. J Phys Chem, 1967, 71: 2271－2276[DOI]
6 Tjahjono M, Allian A D, Garland M. Experimental dipole moments for nonisolatable acetic acid structures in a nonpolar medium. A combined spectroscopic, dielectric, and DFT study for self-association in solution. J Phys Chem B, 2008, 112: 6448－6459[DOI]
7 Nakabayashi T, Kosugi K, Nishi N. Liquid structure of acetic acid studied by Raman spectroscopy and *ab initio* molecular orbital calculations. J Phys Chem A, 1999, 103: 8595－8603[DOI]
8 Freedman E. The use of ultrasonic absorption for the determination of very rapid reaction rates at equilibrium: application to the liquid-phase association of carboxylic acids. J Chem Phys, 1952, 21: 1784－1790[DOI]
9 Cartwright D R, Monk C B. The molecular association of some carboxylic acids in aqueous solutions from conductivity data. J Chem Soc, 1955, 2500－2503
10 Ng J B, Shurvell H F. A study of the self-association of acetic acid in aqueous solution using raman spectroscopy. Can J Spectrosc, 1985, 30: 149－153
11 Ng J B, Shurvell H F. Application of factor analysis and band contour resolution techniques to the Raman spectra of acetic acid in aqueous solution. J Phys Chem, 1987, 91: 496－500[DOI]
12 Tanaka N, Kitano H, Ise N. Raman spectroscopic study of hydrogen bonding in aqueous carboxylic acid solutions. J Phys Chem, 1990, 94: 6290－6292[DOI]
13 Johnson C M, Tyrode E, Baldelli S, Rutland M W, Leygraf C. A vibrational sum frequency spectroscopy study of the liquid-gas interface of acetic acid-water mixtures: 1. Surface speciation. J Phys Chem B, 2005, 109: 321－328[DOI]
14 Tyrode E, Johnson C M, Baldelli S, Leygraf C, Rutland M W. A vibrational sum frequency spectroscopy study of the liquid-gas interface of acetic acid-water mixtures: 2. Orientation analysis. J Phys Chem B, 2005, 109: 329－341[DOI]
15 Nishi N, Nakabayashi T, Kosugi K. Raman spectroscopic study on acetic acid clusters in aqueous solutions: Dominance of acid-acid association producing microphases. J Phys Chem A, 1999, 103: 10851－10858[DOI]
16 Colominas C, Teixido J, Cemeli J, Luque F J, Orozco M. Dimerization of carboxylic acids: Reliability of theoretical calculations and the effect of solvent. J Phys Chem B, 1998, 102: 2269－2276[DOI]
17 Aquino A J A, Tunega D, Haberhauer G, Gerzabek M H, Lischka H. Solvent effects on hydrogen bonds-a theoretical study. J Phys Chem A, 2002, 106: 1862－1871[DOI]
18 Chocholoušová J, Vacek J, Hobza P. Acetic acid dimer in the gas

phase, nonpolar solvent, microhydrated environment, and dilute and concentrated acetic acid: *Ab initio* quantum chemical and molecular dynamics simulations. J Phys Chem A, 2003, 107: 3086－3092[DOI]

19 Génin F, Quilès F, Burneau A. Infrared and Raman spectroscopic study of carboxylic acids in heavy water. PCCP, 2001, 3: 932－942

20 Takamuku T, Kyoshoin Y, Noguchi H, Kusano S, Yamaguchi T. Liquid structure of acetic acid-water and trifluoroacetic acid-water mixtures studied by large-angle X-ray scattering and NMR. J Phys Chem B, 2007, 111: 9270－9280[DOI]

21 Ouyang B, Howard B J. The monohydrate and dihydrate of acetic acid: A high-resolution microwave spectroscopic study. PCCP, 2009, 11: 366－373

22 Pu L, Wang Q, Zhang Y, Miao Q, Kim Y S, Zhang Z B. Architecture of hydrates and local structure of acetic acid aqueous solution: *Ab initio* calculations and Car-Parrinello molecular dynamics (CPMD) simulations on hydrogen-bonding rings, network, and intra-hydrate protonation in multi-hydrates of acetic acid monomer. Adv Quantum Chem, 2008, 54: 271－295[DOI]

23 Pu L, Sun Y M, Zhang Z B. Hydrogen bonding of hydrates of double acetic acid molecules. J Phys Chem A, 2009, 113: 6841－6848[DOI]

24 Car R, Parrinello M. Unified approach for molecular dynamics and density-functional theory. Phys Rev Lett, 1985, 55: 2471－2474[DOI]

25 CPMD, Copyright IBM Corp 1990-2004, Copyright MPI für Festkörperforschung Stuttgart 1997-2001

26 Becke A D. Density-functional exchange-energy approximation with correct asymptotic behavior. Phys Rev A, 1988, 38: 3098－3100[DOI]

27 Lee C, Yang W, Parr R G. Development of the Colle-Salvetti correlation-energy formula into a functional of the electron density. Phys Rev B, 1988, 37: 785－789[DOI]

28 Zhan C G, Dixon D A. Absolute hydration free energy of the proton from first-principles electronic structure calculations. J Phys Chem A, 2001, 105: 11534－11540[DOI]

29 Zhan C G, Dixon D A. Hydration of the fluoride anion: Structures and absolute hydration free energy from first-principles electronic structure calculations. J Phys Chem A, 2004, 108: 2020－2029[DOI]

30 Cancès M T, Mennucci B, Tomasi J, A new integral equation formalism for the polarizable continuum model: Theoretical background and applications to isotropic and anisotropic dielectrics. J Chem Phys, 1997, 107: 3032－3041[DOI]

31 Cossi M, Barone V, Mennucci B, Tomasi J. *Ab initio* study of ionic solutions by a polarizable continuum dielectric model. Chem Phys Lett, 1998, 286: 253－260[DOI]

32 Mennucci B, Tomasi J, Continuum solvation models: A new approach to the problem of solute's charge distribution and cavity boundaries. J Chem Phys, 1997, 106: 5151－5158[DOI]

33 Frisch M J, Trucks G W, Schlegel H B, Scuseria G E, Robb M A, Cheeseman J R, Zakrzewski V G, Montgomery Jr J A, Stratmann R E, Burant J C, Dapprich S, Millam J M, Daniels A D, Kudin K N, Strain M C, Farkas O, Tomasi J, Barone V, Cossi M, Cammi R, Mennucci B, Pomelli C, Adamo C, Clifford S, Ochterski J, Petersson G A, Ayala P Y, Cui Q, Morokuma K, Malick D K, Rabuck A D, Raghavachari K, Foresman J B, Cioslowski J, Ortiz J V, Stefanov B B, Liu G, Liashenko A, Piskorz P, Komaromi I, Gomperts R, Martin R L, Fox D J, Keith T, Al-Laham M A, Peng C Y, Nanayakkara A, Gonzalez C, Challacombe M, Gill P M W, Johnson B, Chen W, Wong M W, Andres J L, Gonzalez C, Head-Gordon M, Replogle E S, Pople J A. Gaussian 98. Revision A.6. Gaussian Inc. Pittsburgh PA. 1998

34 Frisch M J, Trucks G W, Schlegel H B, Scuseria G E, Robb M A, Cheeseman J R, Montgomery Jr J A, Vreven T, Kudin K N, Burant J C, Millam J M, Iyengar S S, Tomasi J, Barone V, Mennucci B, Cossi M, Scalmani G, Rega N, Petersson G A, Nakatsuji H, Hada M, Ehara M, Toyota K, Fukuda R, Hasegawa J, Ishida M, Nakajima T, Honda Y, Kitao O, Nakai H, Klene M, Li X, Knox J E, Hratchian H P, Cross J B, Adamo C, Jaramillo J, Gomperts R, Stratmann R E, Yazyev O, Austin A J, Cammi R, Pomelli C, Ochterski J W, Ayala P Y, Morokuma K, Voth G A, Salvador P, Dannenberg J J, Zakrzewski V G, Dapprich S, Daniels A D, Strain M C, Farkas O, Malick D K, Rabuck A D, Raghavachari K, Foresman J B, Ortiz J V, Cui Q, Baboul A G, Clifford S, Cioslowski J, Stefanov B B, Liu G, Liashenko A, Piskorz P, Komaromi I, Martin R L, Fox D J, Keith T, Al-Laham M A, Peng C Y, Nanayakkara A, Challacombe M, Gill P M W, Johnson B, Chen W, Wong M W, Gonzalez C, Pople J A. Gaussian 03. Revision C.02. Gaussian Inc. Wallingford CT. 2004

35 Boys S F, Bernardi F. The calculation of small molecular interactions by the differences of separate total energies. Some procedures with reduced errors. Mol Phys, 1970, 19: 553－566[DOI]

36 Gao Q, Leung K T. Hydrogen-bonding interactions in acetic acid monohydrates and dihydrates by density-functional theory calculations. J Chem Phys, 2005, 123: 074325[DOI]

37 Pu L, Miao Q, Xu H L, Zhang L L, Zhang Z B. Perception of hydrogen bonding ring in a local structure of aqueous solution in the CPMD simulation (in Chinese). Comput Appl Chem, 2007, 24: 1324－1328